JOURNAL OF GEOPHYSICAL RESEARCH, VOL. 96, NO. D3, PAGES 5055–5071, MARCH 20, 1991

Three-Dimensional Simulations of Wintertime Ozone Variability in the Lower Stratosphere

RICHARD B. ROOD, ANNE R. DOUGLASS, AND JACK A. KAYE

Atmospheric Chemistry and Dynamics Branch, NASA Goddard Space Flight Center, Greenbelt, Maryland

MARVIN A. GELLER AND CHI YUECHEN

Institute for Terrestrial and Planetary Atmospheres, State University of New York at Stony Brook

DALE J. ALLEN, EDMUND M. LARSON, ERIC R. NASH, AND J. ERIC NIELSEN

Applied Research Corporation, Landover, Maryland

The evolution of ozone has been calculated for the winters of 1979 and 1989 using winds derived from our stratospheric data assimilation system (STRATAN). The ozone fields calculated using this technique are found to compare well with satellite-measured fields for simulations of 2–3 months. Here we present comparisons of model fields with both satellite and sonde measurements to verify that stratospheric transport processes are properly represented by this modeling technique. Attention is focussed on the northern hemisphere middle and high latitudes at the 10-hPa level and below, where transport processes are most important to the ozone distribution. First-order quantities and derived budgets from both the model and satellite data are presented. By sampling the model with a limb-viewing satellite and then Kalman filtering the "observations" of the model, it is shown that transient subplanetary-scale features that are essential to the ozone budget are missed by the satellite system.

INTRODUCTION

To understand the behavior of ozone in the stratosphere, it is necessary to evaluate both the transport and photochemical terms of the ozone continuity equation. The transport terms can be calculated using wind fields derived from either general circulation models (GCMs) or data. Models offer the advantage of providing a completely consistent data set for winds and temperatures, but have the disadvantage that simulations of the stratosphere are not quantitatively accurate.

General circulation models of the middle atmosphere are plagued by a series of persistent problems [*Mahlman and Umscheid*, 1984; *Geller*, 1984]. These include the cold pole problem (i.e., simulated stratospheric temperatures at the winter pole being much colder than observations) and lack of interannual variability. In a series of experiments with the SKYHI model, *Mahlman and Umscheid* [1987] showed that the cold pole problem became systematically less severe as the horizontal resolution was increased. This was attributed to the resolution of gravity waves in the GCM. *Hayashi et al.* [1989] confirmed that an important part of the momentum budget in the model is in fact associated with gravity waves. They also point out that the observations by *Fritts and Vincent* [1987] indicate that gravity waves with spatial scales too small to be resolved even by the highest resolution presented by *Mahlman and Umscheid* [1987] play a crucial role in the middle atmosphere momentum budgets. From this modeling experience, it has been concluded that the behavior of both planetary scales and the mean flow are profoundly affected by small-scale processes. Proper inclusion of gravity wave effects is necessary for an accurate simulation of climate.

Two strategies have evolved to address small-scale processes in stratospheric GCMs, both of which impact constituent modeling. The strategy of *Mahlman and Umscheid* [1987] is to resolve gravity waves explicitly (with *Smagorinsky* [1963] nonlinear diffusion for subscale momentum closure in the model). However, even with the 1° version of the SHYHI model, significant differences exist between model and observed monthly mean wind and temperature fields [*Mahlman and Umscheid*, 1987]. Furthermore, to calculate the behavior of reactive constituents at such high resolution is prohibitively expensive.

The second strategy is to parameterize gravity wave processes and add them to coarser resolution models [e.g., *Rind et al.*, 1988]. However, at the present time there is insufficient knowledge of gravity wave sources and gravity wave interactions with the mean flow, and therefore gravity wave parameterizations are commonly treated as adjustable parameters. Thus, while the incorporation of subscale parameterizations can improve the comparison of model temperature and wind fields with data, it is not clear how such parameterizations affect constituent transport [see *Mied and Lindemann*, 1984, Figure 4].

The alternative to using model wind fields to understand constituent transport is to use data. However, there are very few direct wind data for the stratosphere, and wind estimates must generally be derived from geopotential heights. Calculations of constituent variability using geostrophic winds derived from height fields are accurate only in a time-averaged qualitative sense. Due either to inaccuracies of the geostrophic approximation or the presence of noise, calcu-

Paper number 90JD02537.
0148-0227/91/90JD-02537$05.00

lated changes are frequently poor approximations of observed changes. Calculations using more sophisticated balanced winds [e.g., *Randel*, 1987] suffer similar problems. The calculation of constituent budgets from satellite data has been discussed by *Douglass et al.* [1985], *Douglass and Rood* [1986], and *Rood et al.* [1989].

In this paper, data assimilation techniques are used to combine general circulation modeling and meteorological data. This produces global analyses of atmospheric winds and temperatures that are constrained by the strong physical requirements of the primitive equations in the GCM. The GCM, however, is never allowed to run long enough that climatological model biases come to dominate the wind fields. This approach has the advantage that by examining periods for which satellite-measured constituent fields are available, the evolution of calculated fields may be directly compared with the evolution of the measured fields [see also *Geller et al.*, 1989].

Rood et al. [1989, 1990*a*] have shown the potential of using winds from a data assimilation to calculate constituent transport. These relatively short studies of HNO_3 behavior established that winds from the assimilation provide enough information to capture day-to-day HNO_3 variability which is primarily of dynamical origin. However, due to possible missing nitric acid chemistry, longer simulations diverged from the limb infrared monitor of the stratosphere (LIMS) observations, so that the full capabilities of the transport calculation could not be examined.

A major point of these earlier studies is that the current meteorological data set contains enough information to represent wintertime stratospheric transport on what might be called a macroscopic scale. That is, the gross observable features of the constituent evolution can be modeled with winds from a data assimilation model. Although the dynamics model is of relatively low horizontal resolution and no gravity wave parameterization is included, the data constraints acting on the model produce transport winds that are consistent with those in the atmosphere. Using this approach, realistic transport calculations can be performed in a three-dimensional chemical and transport model (CTM) at resolutions that are not prohibitively expensive on current computers.

This paper presents results from ozone transport experiments for 1979 (January 1 to February 28) and 1989 (December 28, 1988 to March 31, 1989). The following will be addressed in this paper: (1) refinements of the technique of application of assimilated data to transport experiments, (2) verification that realistic transport can be calculated on seasonal scales, (3) through consistent comparisons with satellite data, why these realistic simulations are possible at such coarse resolutions.

MODEL

Model Characteristics

The modeling method is to take winds from the data assimilation and use them as input in an offline CTM. There is no feedback between calculated ozone and temperature. This approach parallels that described by *Mahlman and Moxim* [1978] and used by other modeling groups [e.g., *Grose et al.*, 1987]. Once initialized, with no additional information concerning observed constituent behavior, the constituent fields evolve consistently with the wind fields and the chemical formulation. The transport model extends from the ground to 55 km and is global in domain. The data assimilation system, STRATAN, is described more fully by *Rood et al.* [1989, 1990*b*], *Baker et al.* [1987], and *Takano et al.* [1987].

Different transport algorithms are used for the 1979 and 1989 calculations. The spectral transport scheme, with rhomboidal 30 horizontal resolution, is used for the 1979 ozone calculations and is the same scheme used for the HNO_3 simulations [*Rood et al.*, 1989, 1990*a*]. For the 1989 calculations the grid point scheme of *van Leer* [1974] is used with horizontal resolution of 2° latitude by 2.5° longitude.

Van Leer's scheme is representative of a class of upstream-biased, monotonic schemes [*Rood*, 1987] and offers numerous advantages over the spectral method. Most notably, the spectral method is not monotonic and therefore can generate unrealistic overshoots (mixing ratios higher than in the initial field) and undershoots (negative mixing ratios). The negative mixing ratios require filling. The filtering and filling process is constituent dependent and corrupts the correlations between constituents. A scheme that correctly maintains the relationship between constituents is necessary because constituent correlations provide a powerful tool for interpretation of data from the Airborne Arctic Stratospheric Expedition (AASE) [*Fahey et al.*, 1990].

A second major advantage is that the vertical velocity calculation is more localized in space for the grid point scheme than for the spectral scheme. This is a valuable attribute because of the presence of small-scale structures that are not well represented with the global basis functions in the spectral method. The spectral application to the assimilated data can lead to local violations of continuity. Details concerning the adaptation of this transport scheme are given by D. J. Allen et al. (Application of a monotonic upstream transport scheme to three-dimensional constituent calculations, submitted to *Monthly Weather Review*, 1990; hereinafter referred to as submitted manuscript).

The van Leer scheme was implemented for the 1989 experiments after constituent experiments using the spectral scheme showed obvious local violations of continuity after relatively short periods of integration. These were attributed to small-scale structure, which is both real and spurious, present in the 1989 STRATAN fields, which resulted from the input of large amounts of satellite data to the assimilation. Such structures are less pronounced in the 1979 assimilation fields. The 1979 experiments have not been repeated because the cost is high and the results discussed here are expected to be comparable for both transport schemes.

In both transport models the continuity equation is solved by process splitting [*Rood*, 1987; *McRea et al.*, 1982]. The transport algorithm is applied to the constituent field first. Then the transported field is acted upon by the chemistry operator. In these experiments the transport and chemistry time steps are the same. For any constituent the continuity equation is

$$\frac{\partial \chi}{\partial t} = \mathbf{v} \cdot \nabla \chi + P - L\chi \tag{1}$$

where P and L are 15-day averaged values of the 24-hour averaged photochemical production and loss frequency. The advection terms are evaluated to produce an intermediate

constituent field χ^*; the photochemical terms are accounted for by writing (1) as a difference equation:

$$\frac{\chi(t) - \chi(0)}{\Delta t} = \frac{[\chi^* - \chi(0)]}{\Delta t} + P - L\chi(t)$$

and solving

$$\chi(t) = (\chi^* + P\Delta t)/(1 + L\Delta t)$$

For short photochemical time scales ($L\Delta t \gg 1$), this reduces to the photochemical equilibrium limit $\chi(t) = P/L$. The values of P and L are 15-day averages of the 24-hour averaged production and loss frequency and are taken from the GSFC two-dimensional model [*Douglass et al.*, 1989]. The odd oxygen production is given in Figure 1*a*; the odd oxygen loss and the lifetime (loss^{-1}) are given in Figures 1*b* and 1*c*.

Single constituent experiments with zonally and temporally averaged photochemical terms are considered for two reasons. First, this approach is versatile enough that numerous experiments can be run. Our interactive chemistry package [*Kaye and Rood*, 1989] is too expensive to allow adequate experimentation with the transport formulation. Second, the focus of this research is the transport representation in the lower stratosphere during winter. Since the ozone chemical time scales are long for these experiments, and given that the chemical time scales are approximately correct, the details of the chemistry will be of secondary consequence.

Initialization of the O_3 fields is very important for these integrations. The 1979 experiments are initialized with LIMS data above 100 hPa; below 100 hPa, fields are taken from the two-dimensional (2D) model. For the 1989 experiments there are no suitable data for model initialization. Therefore a technique has been developed to generate three-dimensional (3D) initial fields from 2D model results [*Douglass et al.*, 1990]. In this technique, profiles from the 2D model are selected to characterize polar, middle latitude, and tropical air. For each profile, the altitude dependence is expressed as a function of potential temperature. The function for a particular latitude and longitude is then selected based on the potential vorticity at that point. This initialization technique has been verified by comparison with data from LIMS, total ozone mapping spectrometer (TOMS), and AASE.

Winds

The winds for these experiments are taken from the stratospheric data assimilation system STRATAN. STRATAN analyzes wind and geopotential height data at 6-hour intervals on a 4° latitude by 5° longitude grid from the ground to 55 km. The basic technique of data assimilation is to meld a "first-guess field" with the current observations in an optimal fashion to produce an "analysis." The first-guess field is a 6-hour forecast provided by the GCM. The analysis is produced by combining the first-guess field and observations using an objective statistical algorithm. The analysis then becomes the initial condition for the next 6-hour forecast.

Data sources for STRATAN include rawinsondes, surface stations, satellites, buoys, rocketsondes, dropwindsondes, balloons, ships, and aircraft. In the assimilation for 1979 the LIMS temperature profiles are used. Normally, however, only NOAA operational satellite profiles are used. Therefore the standard satellite temperature data are retrievals produced by the National Environmental Satellite Data and Information Service of the TIROS Observational Vertical Sounder (TOVS) radiances. In 1979 data from the vertical temperature profile radiometer are also used.

There is noise associated with any data analysis procedure. The manner in which the assimilation treats noise is crucial to the performance of the transport model. There are two types of noise of significance here. The first is noise that exists in the satellite data which is not present in the actual atmosphere. For instance, particularly in the 1979 meteorological data set, the temperature profiles contain unrealistic barotropic structures that extend from the troposphere to the middle and upper stratosphere. These structures are an artifact of the data reduction algorithm and arise because of errors in the geopotential height fields to which the satellite profiles are referenced. These structures are removed in the data assimilation integration because there is no physical basis in the governing equations to maintain them. Therefore the data assimilation procedure provides a method of noise control.

On the other hand, the data assimilation procedure can create its own noise. As data are melded with the first-guess field, there are local changes to the independent model variables of velocity and temperature. These changes disturb the balance of the model and are therefore a source of small-scale (gravity wave) structure. These structures are generally not real, and when they are real, there is not enough model resolution to treat them correctly. As the forecast progresses, this noise is either damped out or propagates out of the system.

At every 6-hour time interval there are two global fields available: the 6-hour forecast (first guess) field and the analysis. Either field could be used to drive the CTM. While the analysis field compares best with the rawinsonde input data, the 6-hour forecast field compares nearly as well and has the advantage that noise control is provided by the forecast procedure.

Because the ozone experiments using 6-hour forecast winds compare better with observations than those using analysis winds, the 6-hour forecast winds are used for the experiments reported here. The impact of the wind specification is largest at tropical and subtropical latitudes, where a significant bias develops between the simulations and the observations. This will be discussed more fully later.

RESULTS

1979 Winter

There was a wave 1 minor warming in late January 1979 and a wave 2 major warming in late February. These warmings have been studied extensively [e.g., *Leovy et al.*, 1985; *Rood et al.*, 1990*a* and references therein], and no discussion of the dynamical fields will be presented here. Time series and synoptic maps of the model results will be compared with LIMS data. Finally, budgets from both LIMS and the model will be compared and contrasted.

Time Series

Figure 2 shows time series for a simulation that was initialized January 1, 1979, and integrated through the end of

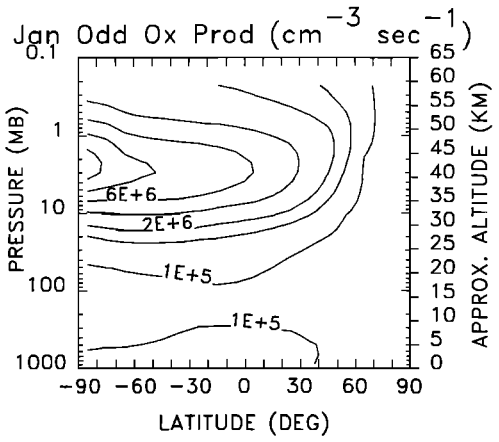

Fig. 1*a*. Photochemical production term for odd oxygen (= ozone below 45 km) for January.

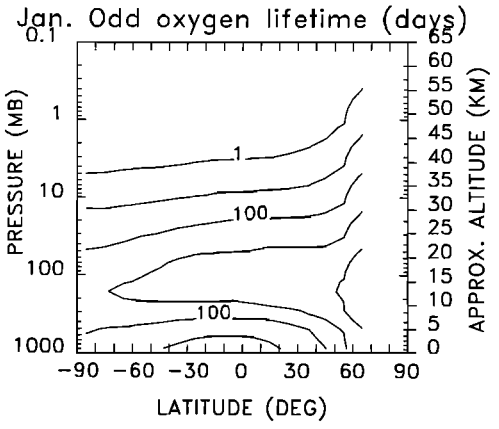

Fig. 1*c*. Loss time scales (inverse of Figure 1*b*).

February. The figure shows zonal mean values at four latitudes and three heights which cover the extratropical northern hemisphere, lower stratosphere. The solid lines are the model values, and the dashed lines are the LIMS data at the two latitudes closest to the model grid point. There has been no space or time filtering of the model output.

At the 100-hPa level, which lies between the lowest stratospheric pressure level and the highest tropospheric level, there is good agreement in the general tendency of model ozone at all latitudes. The bias between the model and data at initialization exists because the 100-hPa level has been interpolated from model levels at 91 and 150 hPa. The 91-hPa level is initialized from LIMS data, and initial values for the 150-hPa level are taken from the 2D model. This bias is therefore due to errors in the 2D model part of the initialization procedure. At 75°N, all of the major events in the LIMS data are represented by the model, but the model shows significantly more time variability. At 60°N the magnitude of the time variability in the model is closer to that seen in LIMS. At 30° and 45°N the general tendency and the reduced amount of time variability are consistent with the observations.

These results suggest that the model credibly represents ozone transport in the very lowest part of the stratosphere.

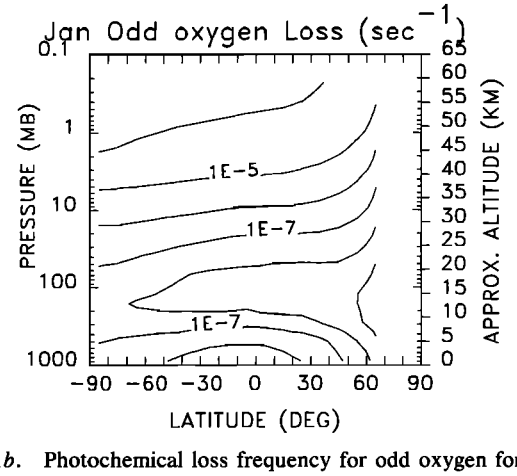

Fig. 1*b*. Photochemical loss frequency for odd oxygen for January.

The differences between the model and the observations are surprisingly small, considering that errors in the LIMS measurements are quite large at this altitude. Furthermore, significant space and time smoothing is imposed by the Kalman filter used in the LIMS analysis (*Remsberg et al.* [1986]; see synoptic representation subsection below). The model fields show much more structure at 100 hPa than the LIMS data. There is an obvious influence of tropospheric disturbances in model values, which will be discussed further.

At 30 hPa the time variability in the model ozone fields is less, thus giving better comparisons with the LIMS data. Except at 30°N the model accurately captures the structure of the observations, but higher frequency time variability remains in the model results. At 30°N, 30-hPa model ozone drifts systematically to lower values. The chemical time scales at this altitude are of the order of 100 days; therefore most of this drift must be due to dynamical processes.

This drift is affected by the wind specification. In Figure 3*a*, ozone is shown at 50 hPa from the same experiment reported in Figure 2; the results from an experiment that is identical, except analysis winds have replaced the 6-hour forecast winds, are shown in Figure 3*b*. Both frames show a drift in the model, but the drift is more obvious in Figure 3*b* where the analysis winds are used. At higher latitudes the differences between the two experiments are much smaller. This drift is largely related to the vertical velocity calculation in the tropics.

At 10 hPa the photochemical time scales are short enough that the specification of the photochemistry becomes important. At both 30° and 45°N the model is approaching the chemical equilibrium values of the 2D model from which the chemistry was derived. The equilibrium values are higher than the observations. At 60° and 75°N the model continues to simulate the dynamical variability accurately. By the end of the integration, however, the high model values at lower latitudes impact the ozone calculated at the highest latitudes of the model.

Synoptic Representation

The zonal mean time series above give some indication of the 2D behavior of the model. The synoptic maps show the longitudinal behavior. Orthographic projections of LIMS data and two representations of model results are given in

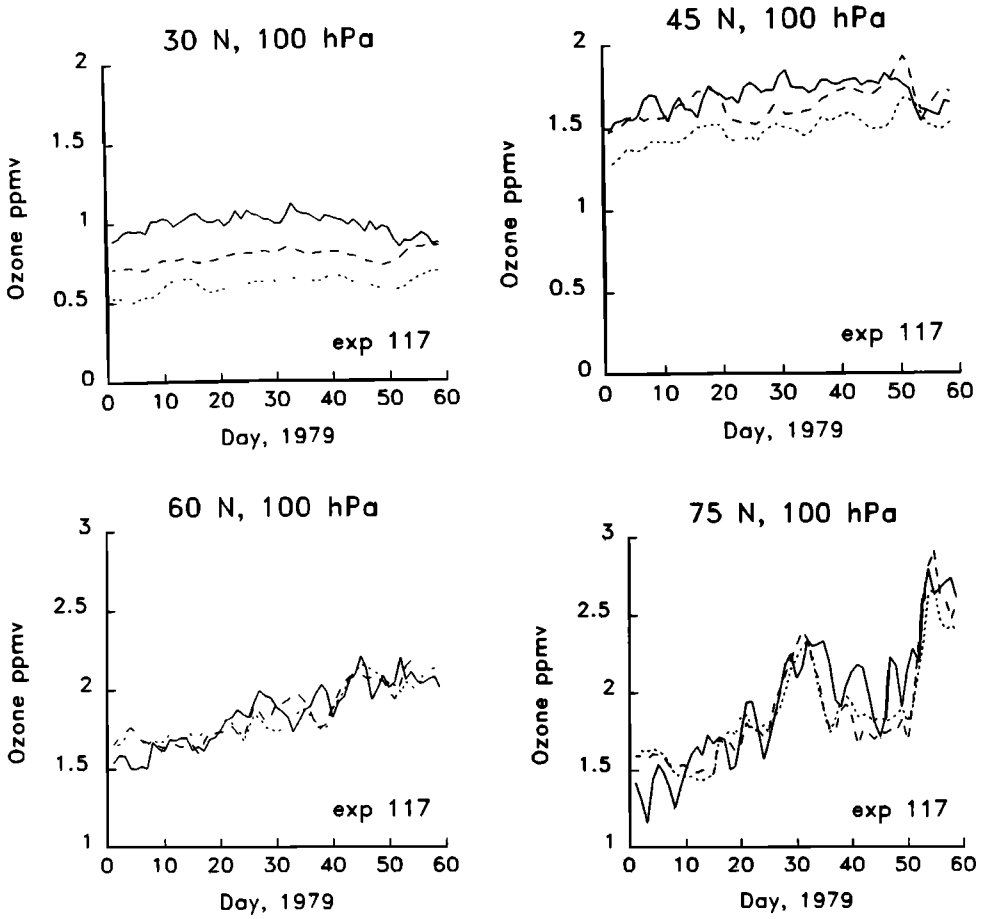

Fig. 2*a*

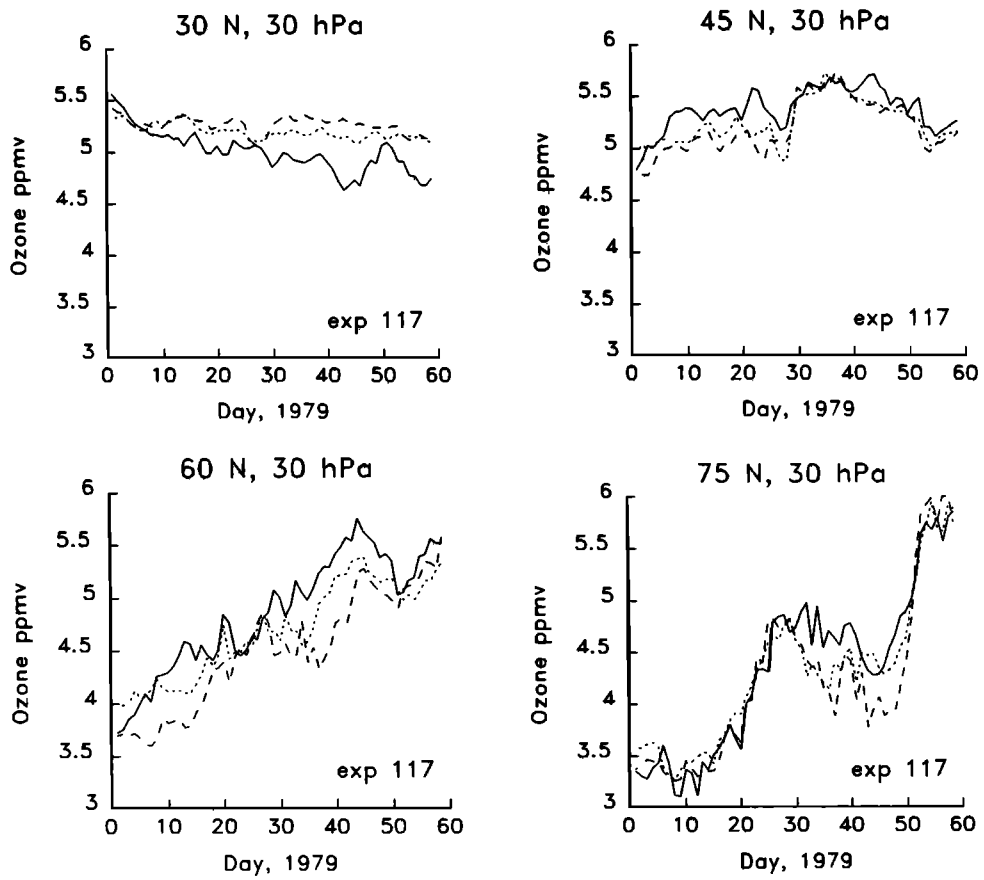

Fig. 2*b*

Fig. 2. Time series of zonal mean ozone from the model (solid curve) and two closest LIMS grid points (dashed curves) (ppmv). Each part has plots for 30°N, 45°N, 60°N, and 75°N: (*a*) 100 hPa, (*b*) 30 hPa, and (*c*) 10 hPa.

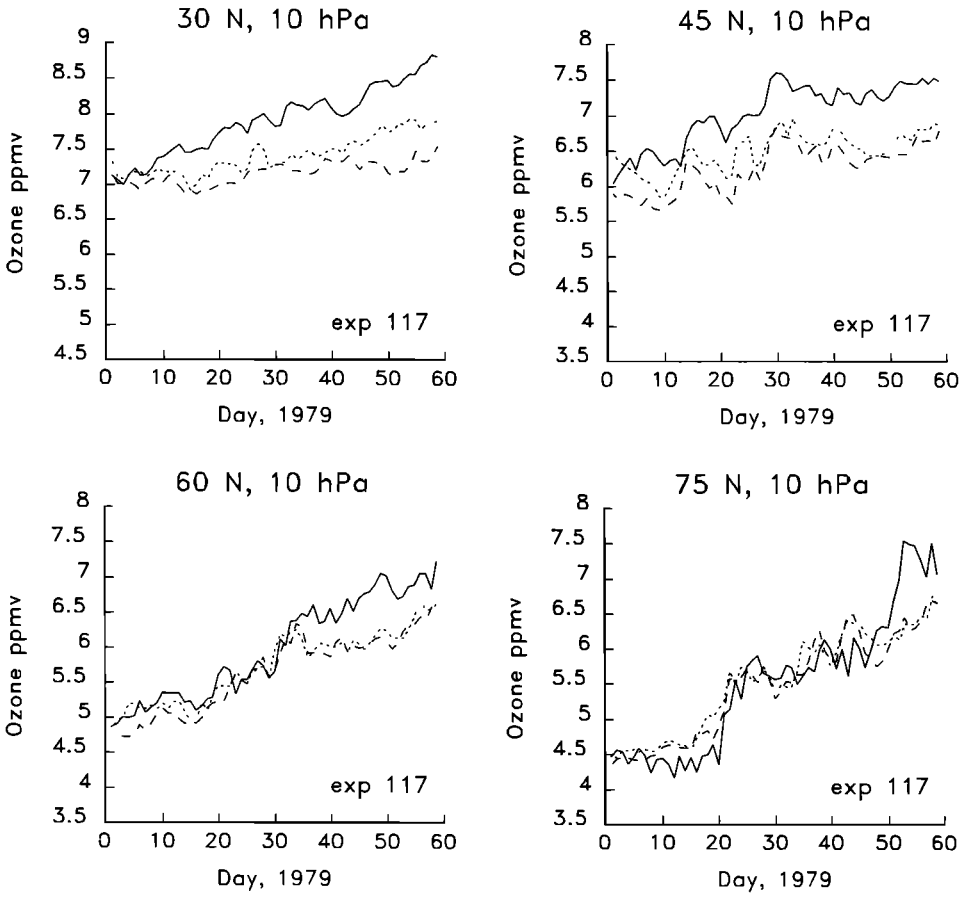

Fig. 2c

Figures 4a–4c. The orthographic projections show data from the equator to the pole, but the area between the equator and 30°N is confined to the edge of the graph. The latitude lines on the map are at 0°, 30°N, and 60°N. The plots are oriented with Greenwich to the right, and increasing longitude counterclockwise.

The two representations from the model are an instantaneous plot of the model fields (Figure 4b) and the field which is produced by applying a Kalman filter to the result of sampling model fields as by a limb-viewing satellite (Figure 4c). An obvious feature of the figure is that the model shows much more variability in the tropics than do the mapped LIMS data. The nature and reality of this tropical variability are not considered in detail in this paper.

Figure 4 is for February 25, 1979, during the wave 2 major warming after 56 days of integration. The polar vortex has split, and high ozone values have propagated over the pole. The agreement between the data and the Kalman-filtered

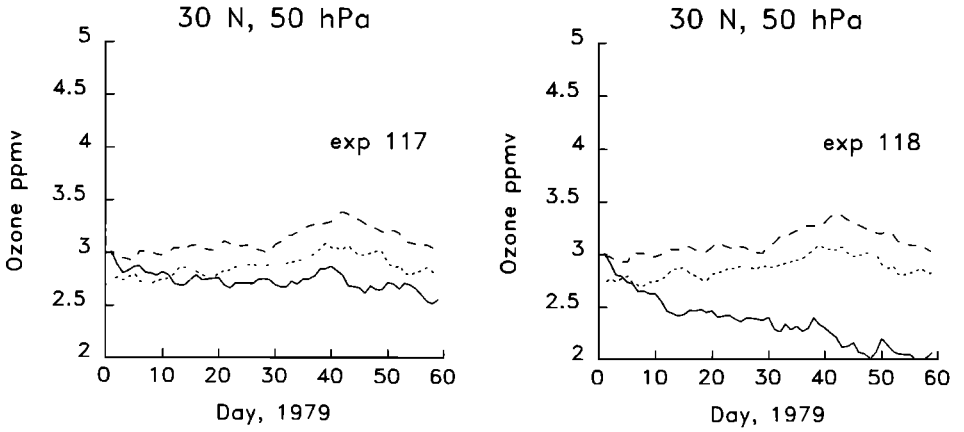

Fig. 3a

Fig. 3b

Fig. 3. Same as Figure 2 except 30°N, 50 hPa. (a) Same experiment as Figure 2. (b) Same experiment except analysis winds are used instead of 6-hour forecast winds (see text, section on winds).

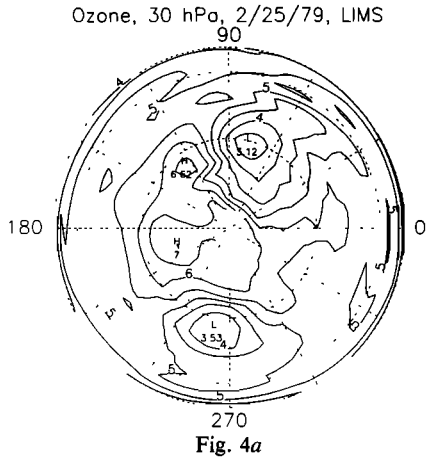

Fig. 4*a*

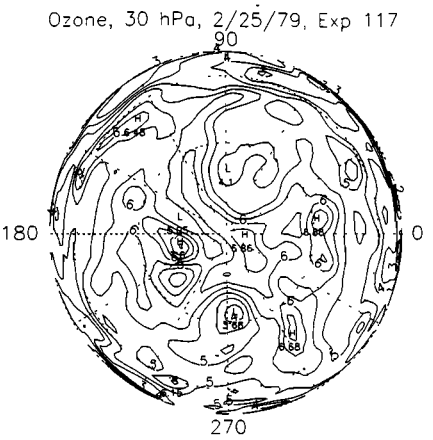

Fig. 4*b*

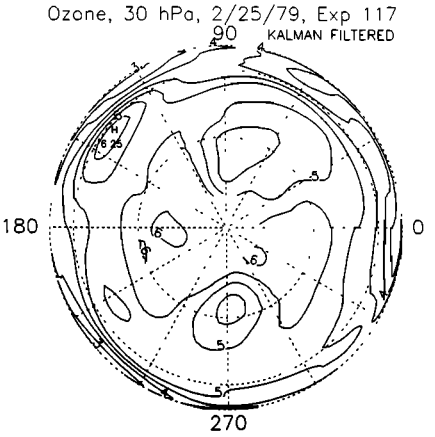

Fig. 4*c*

Fig. 4. Ozone at 30 hPa on February 25, 1979 (ppmv). (*a*) LIMS data. (*b*) Model at synoptic time 12 GMT. (*c*) Model observed by a limb-viewing satellite and the simulated observations Kalman filtered

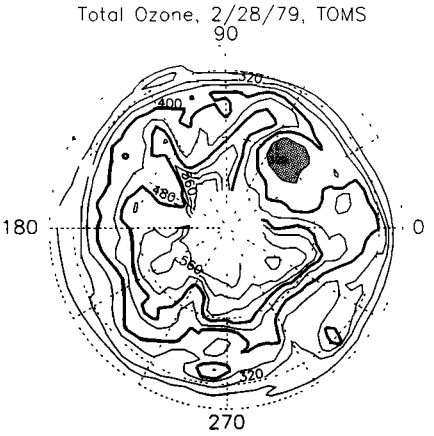

Fig. 5*a*

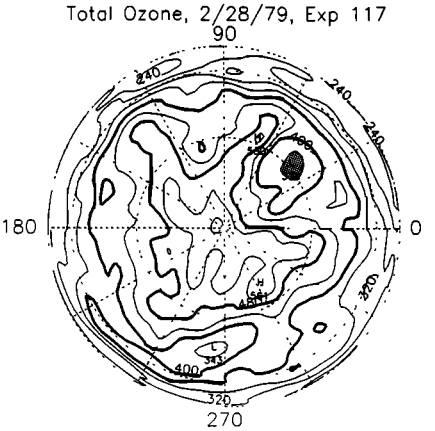

Fig. 5*b*

Fig. 5. Total ozone on February 28, 1979 (Dobson units). (*a*) TOMS data. (*b*) Model.

model results is much better than the agreement between the data and the synoptic map. Both the model and the data show a distinctly split polar vortex which is characterized by low values of ozone; however, the LIMS data have deeper lows. The structure of the high that has replaced the low polar values is accurately captured by the model.

A feature of particular note is the high-low couplet seen between 180° and 240°E, 60° and 75°N in Figure 4*b*. This feature shows values as high as 7.5 ppmv and as low as 4.5 ppmv. This feature is not identifiable in the LIMS data (Figure 4*a*) or in the Kalman-filtered model data (Figure 4*c*). Such features are always present in the model simulation and are an integral part of the progression from one synoptic state to another. Information on the space and time characteristics of such features is necessary if budgets are to be calculated accurately, since such features will significantly impact the computations of spatial and temporal deviations. It is the role of a fully nonlinear CTM to provide a representation of these processes.

It was noted above that the 100-hPa results showed much more time variability than the LIMS data. The 100-hPa level is constantly influenced by tropospheric disturbances. The model shows significant tropospheric influence to the 30-hPa level. If the 100-hPa results are sampled and filtered to simulate the satellite measurement and subsequent data processing, then many of these subplanetary-scale transient disturbances are removed, and the model reveals major features that are present in the data. The agreement in the time series discussed above is much better if the model is smoothed with the Kalman filter.

Comparison of column measurements with calculated columns is of limited significance for assessing transport. However, total ozone is strongly influenced by lower strato-

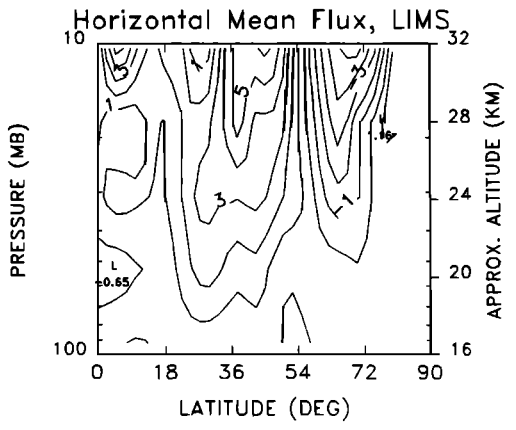

Fig. 6a

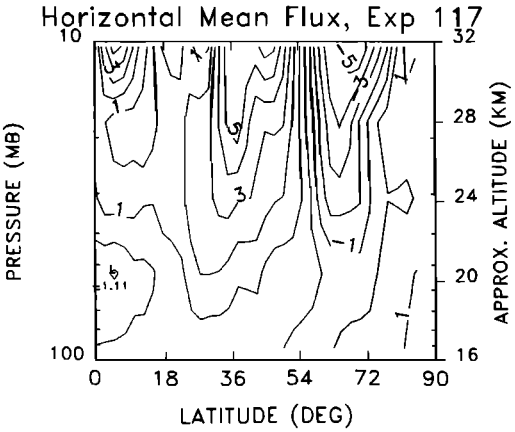

Fig. 6b

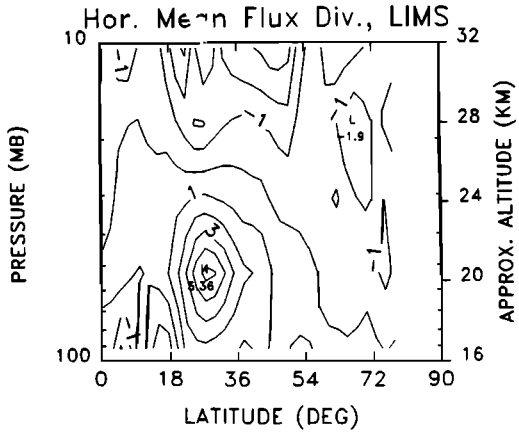

Fig. 6c

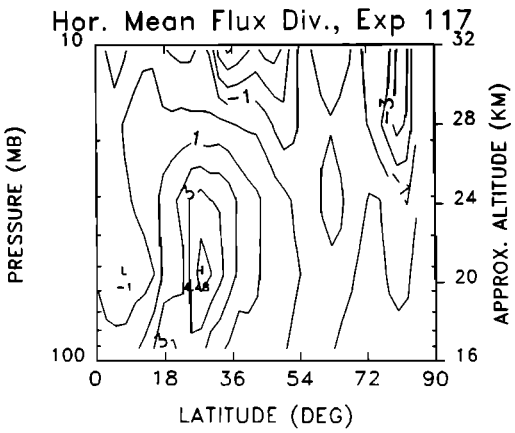

Fig. 6d

Fig. 6. February average budget components of the zonal mean ozone continuity equation for both LIMS data and model. (*a*) LIMS mean meridional flux ($[v][O_3]$). (*b*) Model flux. (*c*) LIMS flux divergence. (*d*) Model flux divergence. Fluxes are in ppmv m s^{-1}, and divergences are in 10^{-2} ppmv d^{-1}.

spheric properties and tropopause behavior; therefore comparison of the model total ozone with the TOMS data provides a measure of the quality of the transport representation for the upper troposphere and lower stratosphere. The model total ozone is compared with TOMS total ozone for February 28, 1979, in Figure 5. The 480 and 400 Dobson unit (DU) contours are defined by heavy lines. At low latitudes the model total ozone is somewhat lower than TOMS, as seen by the presence of the 240 contour in the model total ozone. This is expected because of the systematic bias between the model and data in the time series of Figure 2. At high latitudes the major features of the measurements are all present in the simulation. Of note is the shaded area of low total ozone at 45°E. This is one of the centers of the polar vortex that has split during the warming. The other center is not as distinct in total ozone field as it is in the 30-hPa maps (e.g., Figure 4). The mapping considerations for TOMS/model comparisons are of a different nature than for LIMS/model comparisons. The TOMS maps are not Kalman filtered and are essentially pieced together, quasi-synoptic swaths of observations.

Budgets

Diagnostic budget calculations are a valuable aid for understanding model behavior and defining the differences between model and data. However, the problem of calculating balanced budgets from either satellite data or model history tapes is not as straightforward as it first appears. As shown in Figure 4, the model fields are full of structure that the satellite observing system misses. These transient disturbances are integral to the internal calculations of the model and have time scales of the order of or less than 1 day. Therefore efforts to calculate day-to-day changes from single daily synoptic observations are frequently futile. For this model, synoptic observations (full resolution) separated of the order of 2 hours are needed to provide a meaningful balanced budget calculation [see *Geller et al.*, 1989].

Even though day-to-day balances might be difficult to calculate from synoptic data, spatially and temporally averaged budgets should provide insight into transport processes [e.g., *Wu et al.*, 1987]. The continuity equation for the zonal mean ozone can be written as

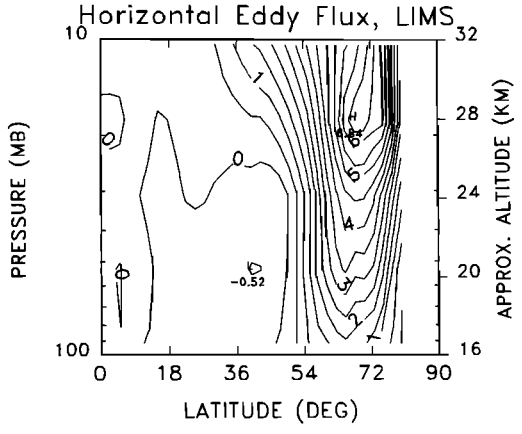

Fig. 7a

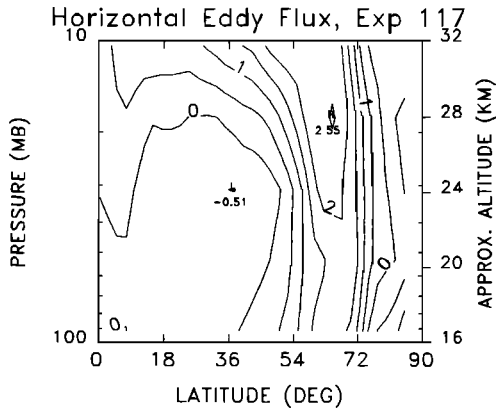

Fig. 7b

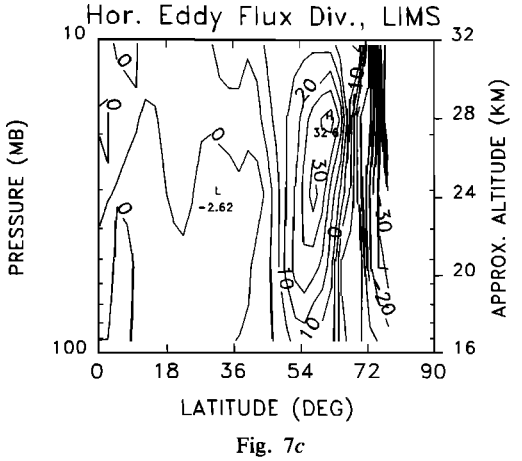

Fig. 7c

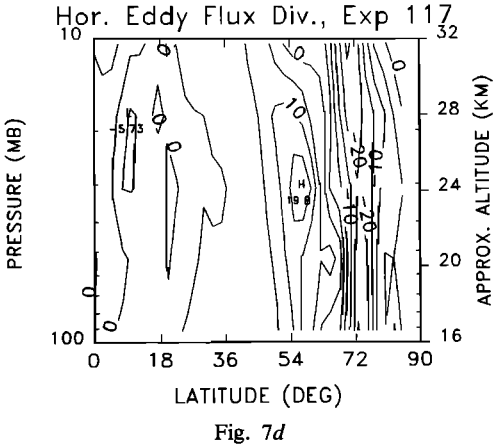

Fig. 7d

Fig. 7. February average budget components of the zonal mean ozone continuity equation for both LIMS data and model. (*a*) LIMS horizontal eddy flux ($[v^*O_3^*]$). (*b*) Model flux. (*c*) LIMS flux divergence. (*d*) Model flux divergence. Fluxes are in ppmv m s^{-1}, and divergences are in 10^{-2} ppmv d^{-1}.

$$\frac{\partial[\chi]}{\partial t} = \nabla \cdot [\mathbf{v}][\chi] - \nabla \cdot [\mathbf{v}^*\chi^*] + [P] - [L\chi]$$

where square brackets represent the zonal mean and asterisks represent the deviations from the zonal mean. The first term on the right is the mean term, and the second term is the horizontal eddy term. The last two terms are the chemical terms and will be ignored here, since the primary focus is the winter lower stratosphere, where the chemical time scales are long.

Figures 6–9 show the flux and flux divergence for each of these four terms for both the model and the LIMS data. Analysis winds from STRATAN were used to calculate the LIMS fluxes. In studies of the Eulerian zonal mean budget, because the planetary waves force a compensating mean meridional circulation, compensation is expected between the mean vertical flux and the horizontal eddy flux.

Examination of the flux divergence terms shows that north of 30° the divergence of the vertical mean flux and the horizontal eddy flux are the two largest terms. They do tend to counterbalance each other, as is expected. Of note, however, is that the balance between these two terms evaluated using data differs considerably from the model balance. The LIMS horizontal eddy flux divergence is noticeably larger than the model divergence. The vertical flux divergence in the model is slightly larger than the divergence in the LIMS data. There is a significant difference in the budget balances.

The mean meridional flux divergence and the vertical eddy flux divergence are smaller than the other two terms. However, neither of the terms are insignificant, and there are places in the atmosphere where they are very important. While there are significant differences in magnitude between the model and LIMS budgets for all the terms, perhaps the most important difference is in the vertical eddy flux term. This is largely due to the model fields having a much more highly developed wave structure (e.g., Figure 4). In the model above 28 km and south of 30°N, the vertical eddy flux divergence provides a decreasing ozone tendency. The magnitude of the terms in the model and the LIMS data show general agreement with the budget studies of *Wu et al.* [1987], who carried out similar calculations using National Meteorological Center temperature profiles together with solar backscatter ultraviolet ozone data.

Both of the mean terms are important in the tropics, where the Hadley circulation is expected to be strong. The model shows a more vigorous circulation than the LIMS data. The vertical winds from STRATAN were used in the budget

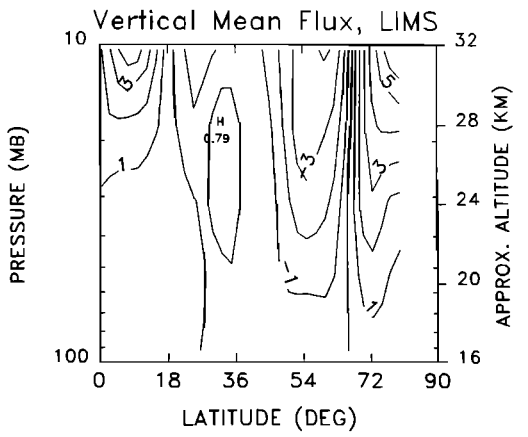

Fig. 8a

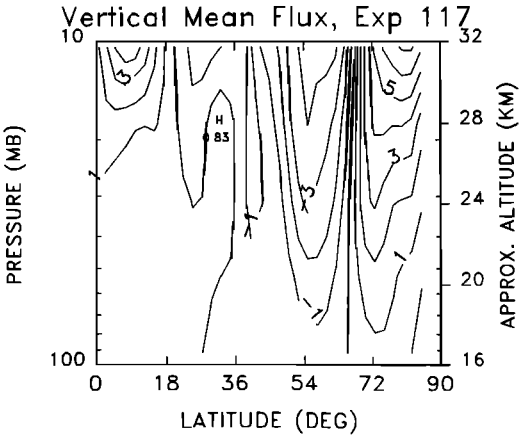

Fig. 8b

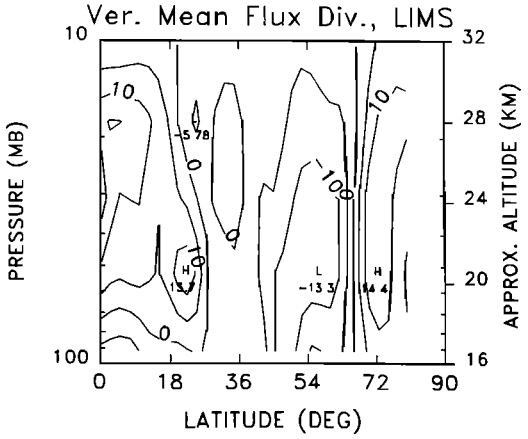

Fig. 8c

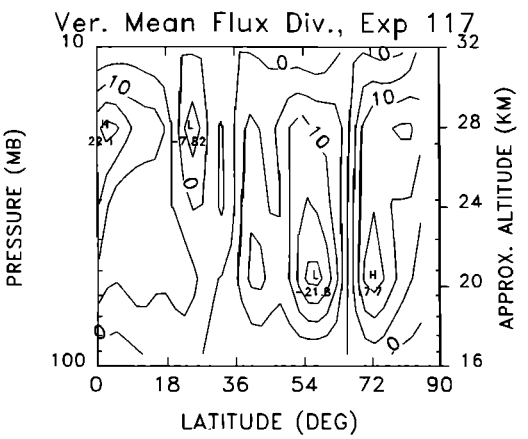

Fig. 8d

Fig. 8. February average budget components of the zonal mean ozone continuity equation for both LIMS data and model. (*a*) LIMS mean vertical flux ($[w][O_3]$). (*b*) Model flux. (*c*) LIMS flux divergence. (*d*) Model flux divergence. Fluxes are in ppmv cm s^{-1}, and divergences are in 10^{-2} ppmv d^{-1}.

calculations. Comparison of these vertical winds to winds derived from diabatic diagnostics [see *Wu et al.*, 1987] shows the STRATAN vertical winds to be larger in the tropics. The model does show a drift relative to the data at low latitudes, which implies that the tropical mean meridional circulation is too strong in the assimilated data.

The differences between the February 1 and February 28 zonal mean ozone fields for both the model and LIMS are shown in Figure 10. The agreement between model and LIMS is quite good, with a decrease in middle latitudes and an increase at high latitudes. Even in the tropics the discrepancies are not too large. However, since the dynamics are tending to decrease ozone above 25 km south of 30°N, much of the increase observed in the model is caused by the chemical processes (see Figure 2*c* and discussion).

1989 Winter

The AASE took place during the winter of 1989. January was characterized by very cold temperatures in the polar vortex. In late January there was a minor warming confined to the upper stratosphere. In the middle of February there was a major wave 2 warming. Several articles discussing the meteorology of the winter of 1989 are contained in *Geophysical Research Letters*, volume 17, number 4, March 1990.

The experiment reported here was initialized on December 28, 1988, and run through March 31, 1989. The initialization procedure is described by *Douglass et al.* [1990]. It should be noted that the initial condition is derived from 2D model calculations, since suitable data are not available. Therefore disagreement between the model and observations is not unexpected. The most complete data available for model verification are from TOMS. While this comparison does not provide as much information as comparison with the vertical information provided by the 1979 LIMS data, the model total ozone field was shown to compare well with the total ozone field for 1979 (Figure 5). Good comparisons between the model and TOMS data provide a measure of the quality of the upper troposphere and lower stratosphere transport representation.

Figure 11 shows four time series of the model and TOMS total ozone at 58°N. Figure 11*a* shows the time series at "Stavanger," Norway (5°E), and the other locations are separated by 90° of longitude. The general tendency of all the time series compares favorably with the TOMS data. Furthermore, the day-to-day variability is of the right scale and

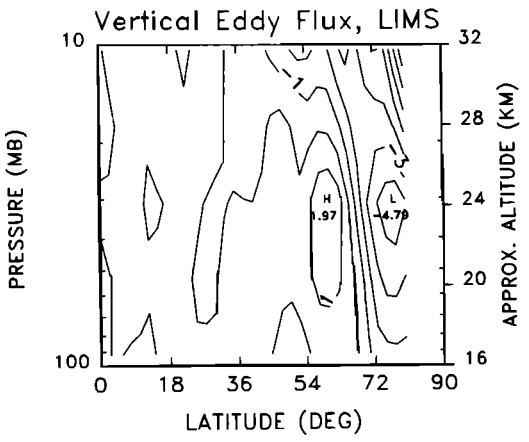

Fig. 9a

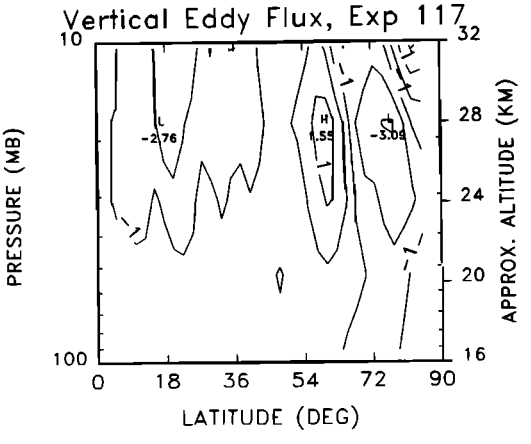

Fig. 9b

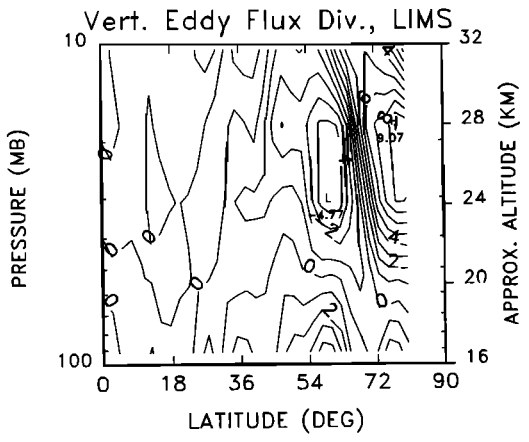

Fig. 9c

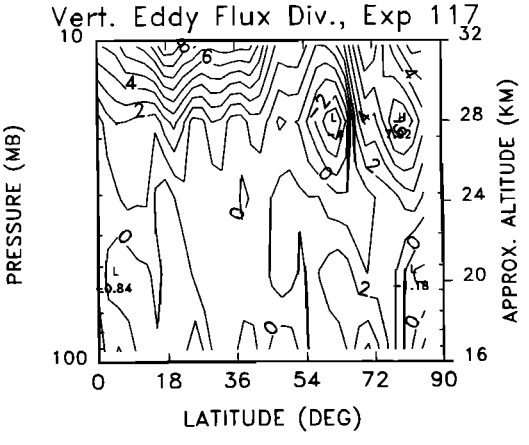

Fig. 9d

Fig. 9. February average budget components of the zonal mean ozone continuity equation for both LIMS data and model. (*a*) LIMS vertical eddy flux ($[w^*O_3^*]$). (*b*) Model flux. (*c*) LIMS flux divergence. (*d*) Model flux divergence. Fluxes are in ppmv mm s^{-1}, and divergences are in 10^{-2} ppmv d^{-1}.

frequently highly correlated with the observations. As was mentioned previously, the TOMS data are not Kalman filtered, and for any one day a map of TOMS data has data separated by up to 24 hours. This will impact the day-to-day comparisons to some degree.

Figure 11*c* is the time series that is taken from the Aleutian anticyclone sector of the globe. Compared to the other three curves, the variance in this time series is small, and the correlation is weak. It is typical of the simulation that in relatively quiescent regions the day-to-day correlations are weakest.

At the other three points there is a major shift in the curve in early February. The total ozone jumps upward at 5° and 95°E. It jumps downward at 275°E. These jumps are associated with the stretching of the polar vortex in the lower stratosphere prior to the wave 2 warming [see *Newman et al.*, 1989]. As the vortex changes, there is a rearrangement of the high total ozone ring that tends to be at the edge of the vortex. This change is not strictly correlated with stratospheric meteorology because of the profound influence that tropospheric disturbances have on total ozone. However, the drop in total ozone at 275°E over the United States is clearly correlated with the stretching of the stratospheric vortex and the low values of total ozone that are typical of the vortex.

Figures 12–15 show model total ozone and TOMS total ozone on January 1, 1989, four days after initialization, and at 1-month intervals. Figure 12 (January 1) is primarily representative of the initial condition, and the major features present in the TOMS data are seen in the model. The large high in total ozone at middle latitudes near 180°E (Aleutian Anticyclone) is well represented. The model total ozone values at middle latitudes are slightly higher than observed, but the shape of the high region surrounding the polar vortex is well represented.

On January 30 (Figure 13) the characteristic signature of wintertime total ozone is seen. A minimum in ozone observed by TOMS and produced by the model appears at 60°N, 0°E. High values of 500 DU are present in the model and simulation at middle latitudes near 150°–180°E. A second area of high ozone appears near 270°E. Even though the magnitudes of the highs are captured quite accurately, the general middle latitude bias remains in the model.

The low values over Scandinavia are the beginning of the late January total ozone minihole (R. B. Rood et al., Episodic total ozone minima and associated effects on hetero-

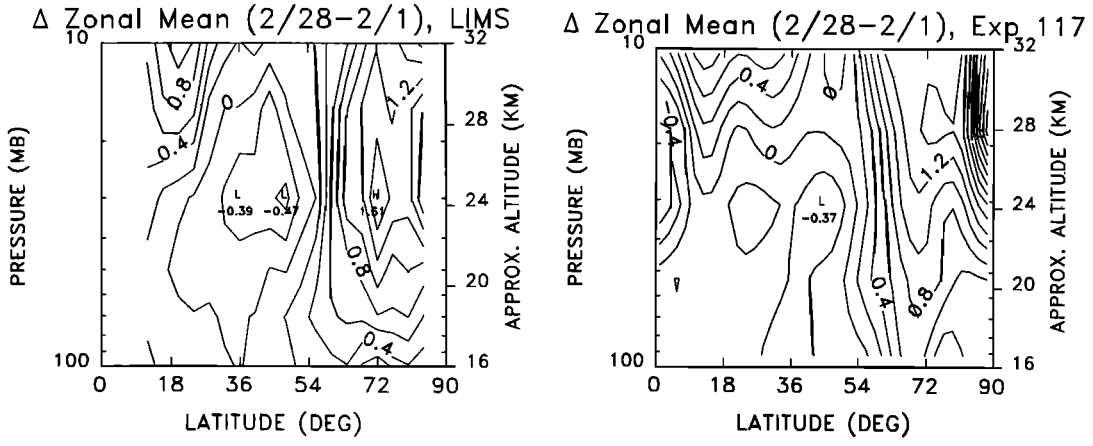

Fig. 10a Fig. 10b

Fig. 10. Difference between zonal mean ozone fields on February 28, 1979, and February 1, 1979 (ppmv). (*a*) LIMS. (*b*) Model.

geneous chemistry and lower stratospheric transport, submitted to *Journal of Geophysical Research*, 1991). The model provides a simulation of this minihole. Since no special chemistry was included to produce the minihole, the minihole must basically be a reversible dynamical event. Otherwise, the low values of ozone displaced toward the Siberian side of the globe are representative of the polar vortex in the stratosphere. Because of polar darkness, there are no TOMS data in this region.

After 2 months of integration (February 28, Figure 14),

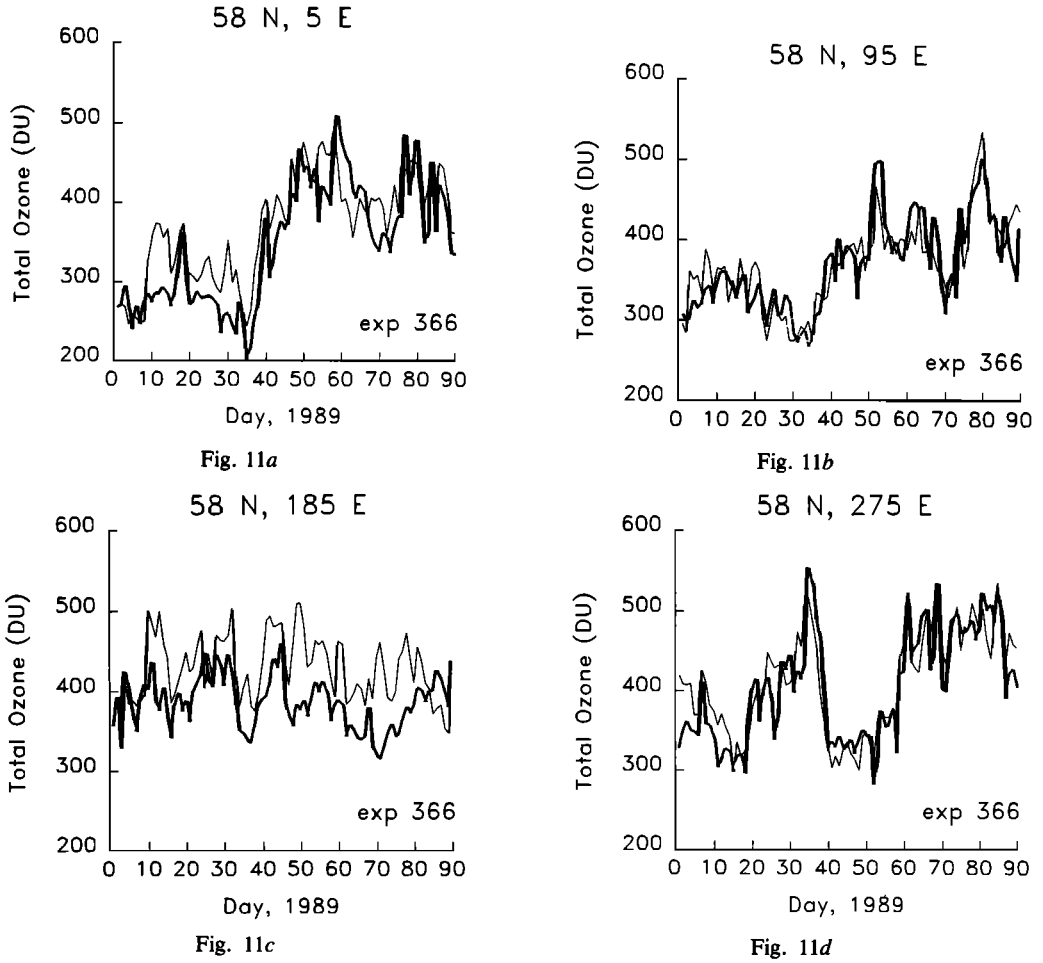

Fig. 11a Fig. 11b

Fig. 11c Fig. 11d

Fig. 11. Time series of TOMS (bold) and model at specified points (Dobson units): (*a*) 58°N, 5°E ("Stavanger"), (*b*) 58°N, 95°E, (*c*) 58°N, 185°E, and (*d*) 58°N, 275°E.

major features in the data are still captured by the simulation. There are areas of high total ozone near 60°N 150°E and near 50°N between 60° and 90°E in both fields. The 440 DU contour, highlighted in both plots, emphasizes the structural similarity of the fields. This figure is after the wave 2 warming, and there has been a major buildup of total ozone at polar latitudes.

During the wave two warming, low values of total ozone were transported out of the vortex (vis a vis Figures 4 and 5 for 1979). These vortex fragments agreed well both in magnitude and location with the TOMS data. Since these fragments had spent most of the winter in polar night and were hence not observed, the agreement in magnitude adds credibility that the model ozone in polar night is, in fact, a good representation of reality.

By the end of March (Figure 15) the clear agreement between observations and data has degraded. The high-low couplet between 270°E and Greenwich is well represented. However, the model high over Siberia is completely absent in the TOMS data. It is difficult to make comparisons near the Pole due to the missing data at the Pole in the TOMS field. The 320 contour is displaced southward in the model compared to TOMS, and the distinction between tropical and middle latitude air is much better defined in the model.

In the comparisons with both the LIMS data and the TOMS data (Figures 2 and 11) there were quantitative differences between the day-to-day variability. Figure 16 shows a comparison of January average total ozone from TOMS and from the model. There are two versions of the model data: a complete version and a version where polar night and other missing data have been removed from the model field. The latter version is shown both to emphasize that the model can provide information in the absence of measurements and to facilitate comparison of model with measurements.

As in the daily synoptic pictures above, there is somewhat more ozone in the model middle latitudes than in the observations. There is good agreement with the location and magnitude of the Aleutian high. Though essentially at the edge of polar night, the low over Scandinavia is also present. The complete model field shows a distinct low in the polar night on the Siberian side of the globe. The high-low pattern yields a monthly mean ozone distribution that is dominated by a zonal wave one.

To more closely examine the local evolution of the simulated ozone, vertical profiles from the model are compared with ozonesonde data. An example which is representative of polar night is shown in Figure 17. In each frame the ozone partial pressure from Heiss Island is given by the thin line, and the heavy line is the nearest model grid point. Because the vertical resolution is coarse (~3.5 km in the stratosphere) and because of the shape preferring characteristic of the transport scheme [*Rood*, 1987] (also, D. J. Allen et al., submitted manuscript, 1990), the model cannot produce the fine layered structure apparent in the ozonesonde profiles. Nevertheless, the prominent features can be compared.

On December 31, 1988, three days after initialization, the model fairly well represents the observed ozone (Figure 17*a*). However, by January 25, 1989 (Figure 17*b*), the model significantly underestimates the ozone partial pressure in the lower stratosphere. This is typical of the profiles from early January through early February, when Heiss Island is confined to the polar vortex [see *Newman et al.*, 1989]. Recent

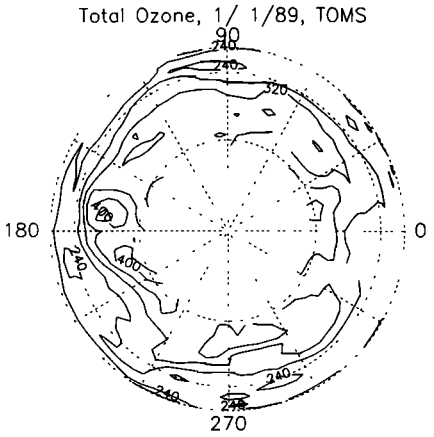

Fig. 12*a*

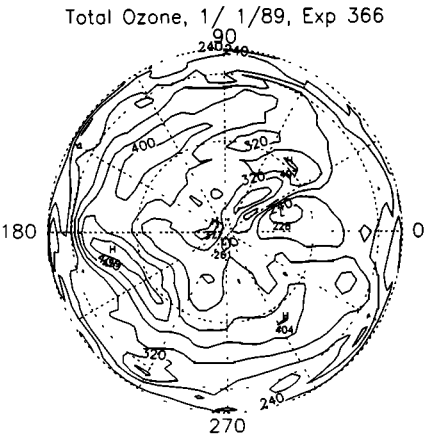

Fig. 12*b*

Fig. 12. Total ozone on January 1, 1989 (Dobson units). (*a*) TOMS. (*b*) Model.

experiments using *Prather*'s [1986] scheme for vertical advection reduces this bias by about 50%. Even though the model is persistently low, day-to-day variability can be followed with some accuracy. Outside of the polar vortex, the model much more faithfully represents the lower stratospheric peak.

On February 18, as the vortex is stretching and splitting during the wave 2 warming, the model reproduces the observed profile. This is due to the ability of the model to represent the advective flux accurately and transport nonvortex air to high latitudes. The model does not capture the magnitude of the extreme increase seen on the next day (Figure 17*d*); however, the model does shift the profile in the right direction. Finally, by March 2, after the ozone has been significantly perturbed, the model has reproduced the basic changes observed in the profile. These comparisons with the sondes show that the model has reproduced the redistribution of ozone in the upper troposphere and lower stratosphere during winter, consistent with the observations.

DISCUSSION

Simulations that reproduce the observed behavior of ozone in the lower stratosphere during winter in the northern hemisphere have been presented. There are two essential

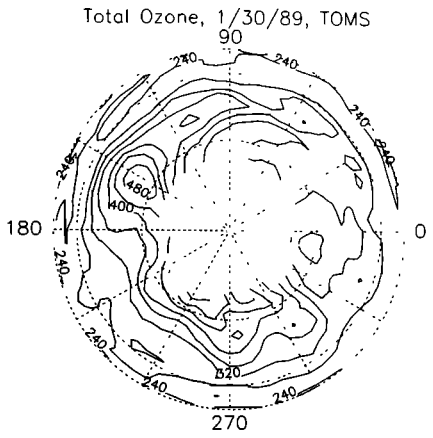

Fig. 13*a*

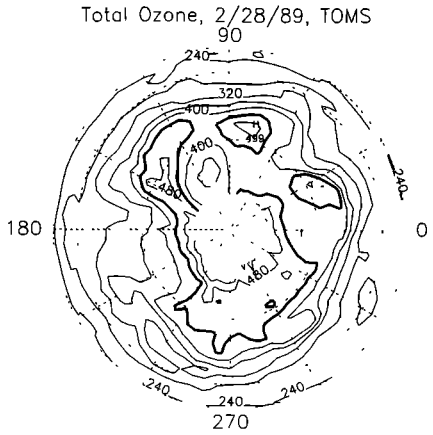

Fig. 14*a*

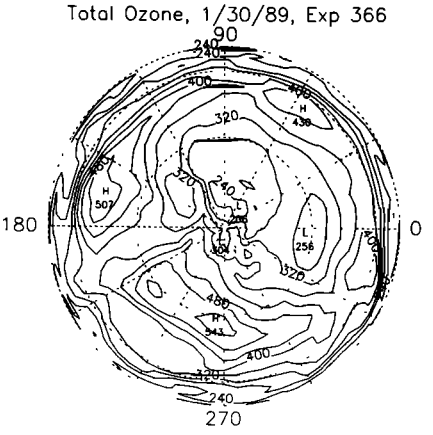

Fig. 13*b*

Fig. 13. Total ozone on January 30, 1989 (Dobson units). (*a*) TOMS. (*b*) Model.

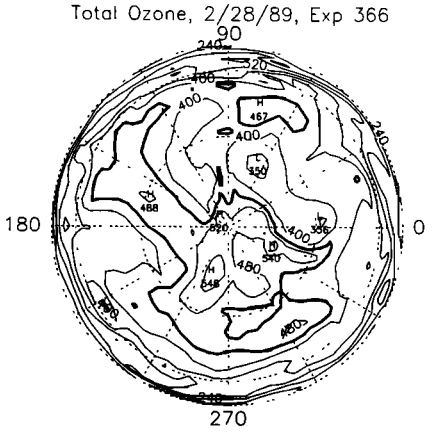

Fig. 14*b*

Fig. 14. Total ozone on February 28, 1989 (Dobson units). (*a*) TOMS. (*b*) Model.

ingredients in producing the realistic simulations presented here: winds from the data assimilation and the 3D chemistry transport model.

By using winds from the assimilation, some of the problems with GCM representations of transport discussed in the introduction have been circumvented. Most notably, realistic simulations of constituent transport have been performed with winds derived from a GCM with moderate to coarse resolution. These results show that at least during wintertime, when Rossby wave dynamics are prominent, there is enough information in the meteorological data to represent transport processes. Simulations of N_2O variability show that it is possible to represent "vortex isolation" [*Loewenstein et al.*, 1990, and references therein] with what appears to be realistic characteristics.

The use of winds from the assimilation has some advantages over the use of a free running GCM. It should be possible to address some fundamental problems of atmospheric transport. For instance, the data from the polar aircraft missions show very low values of long-lived constituents in the wintertime polar vortex. These low values imply descent within the polar vortex. To date, GCMs have been unable to reproduce these low values. This is essentially the constituent manifestation of the cold Pole problem. With winds from the assimilation and careful transport modeling, 3D simulations of setting up constituent distributions within the vortex are possible.

Another fundamental transport problem that can be addressed is interannual variability and the quasi-biennial oscillation. GCMs have not produced adequate simulations of either of these phenomena. Since the dynamics of these events are fundamentally included in the assimilated data, it should be possible to quantify the dynamical mechanisms of interannual variability much more clearly.

More generally, winds from the assimilation plus the availability of global constituent measurements greatly enhance our ability to study dynamics and chemistry. The constituent fields provide a measure of the dynamics and chemistry of the atmosphere that is independent of the meteorological data set. If there is the capability of modeling the transport realistically with some degree of confidence, then the study of how the modeled constituent fields diverge from observations provides an extremely valuable tool to point at the greatest weaknesses in our understanding of atmospheric processes.

Two examples of how this can focus research follow. The first example is that given by *Rood et al.* [1990*a*]. In that paper the geographical distribution of the divergence be-

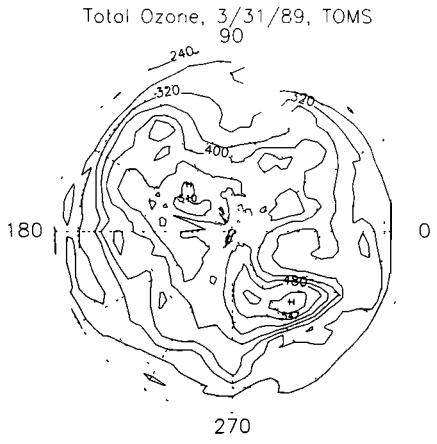

Fig. 15*a*

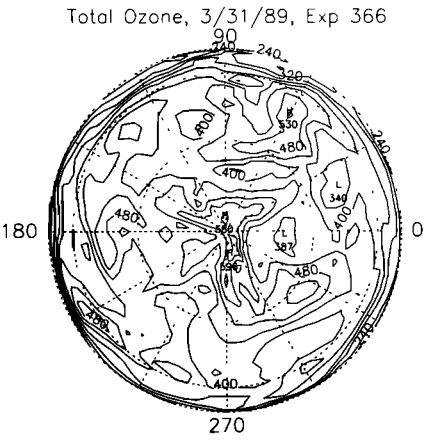

Fig. 15*b*

Fig. 15. Total ozone on March 31, 1989 (Dobson units). (*a*) TOMS. (*b*) Model.

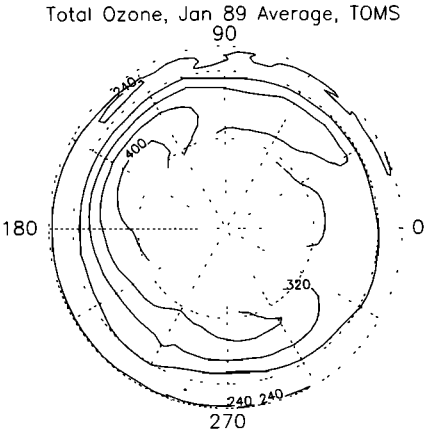

Fig. 16*a*

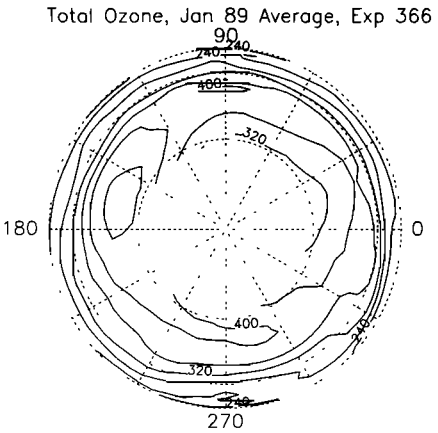

Fig. 16*b*

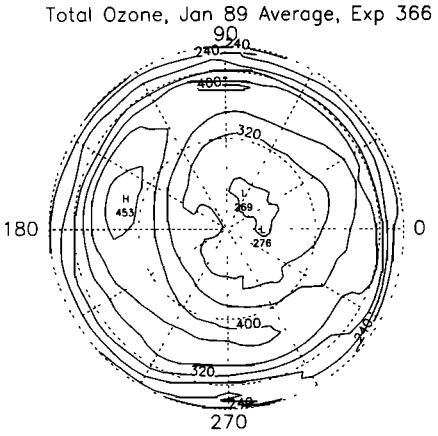

Fig. 16*c*

Fig. 16. Total ozone January 1989 monthly average (Dobson units). (*a*) TOMS. (*b*) Model with polar night removed. (*c*) Full model fields.

tween LIMS HNO_3 and model HNO_3 was used to help better define the shortcomings of wintertime HNO_3 chemistry. The second is contained in this paper, which shows that there are some fundamental problems in our understanding of tropical transport. These problems may be data related or model related. Currently, however, our greatest attention is being focussed on the representation of diabatic processes in the tropics (most particularly, latent heat release in cumulus towers).

These simulations have also shown that the mapped satellite data record is fundamentally lacking in some respects [e.g., *Salby*, 1989]. This is most obvious in Figure 4, where Kalman-filtered model results compare much more closely with the data than the full model field. The model fields are full of subplanetary-scale transient disturbances that are an essential part of the constituent budgets. These subscale features do not merely represent diffusive processes. In this modeling approach the CTM has provided a mechanism to generate a representation of these subscale processes that is consistent with the constituent continuity equation. In other words, the CTM has been used to supplement the data set.

This, of course, provides some intriguing questions about studies that have been based on satellite constituent observations. Figures 6–9 point toward these questions. While the model reproduces the observed ozone behavior with a high degree of accuracy, the balance between the terms in the continuity equation is quite different between model and LIMS. This suggests that the missing information in the satellite data might profoundly impact the understanding of transport processes that have been previously derived with

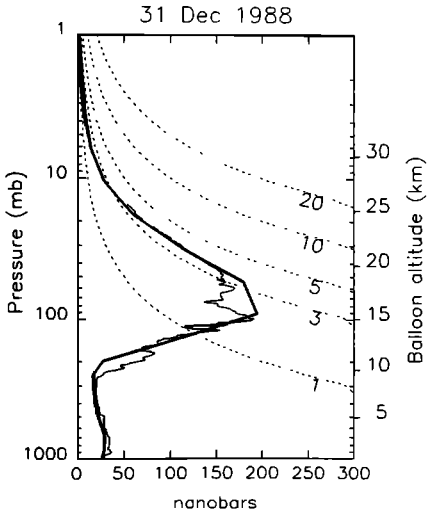

Fig. 17*a*

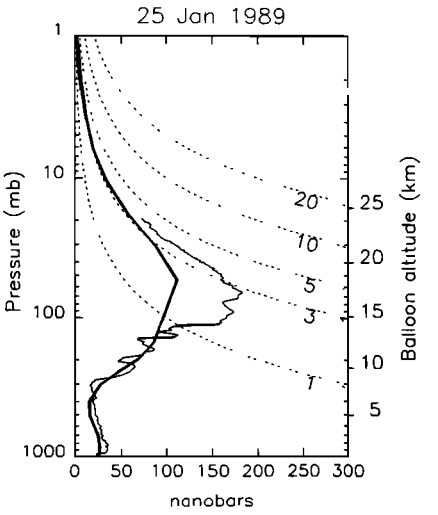

Fig. 17*b*

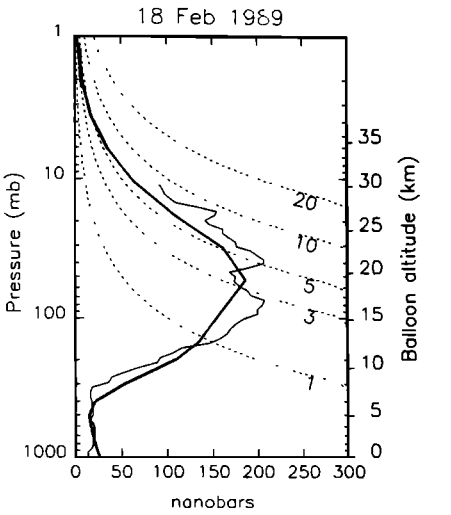

Fig. 17*c*

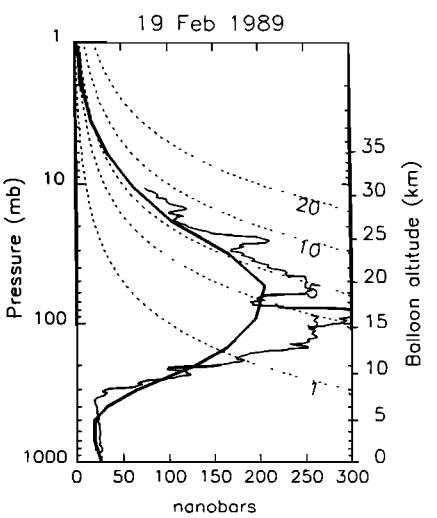

Fig. 17*d*

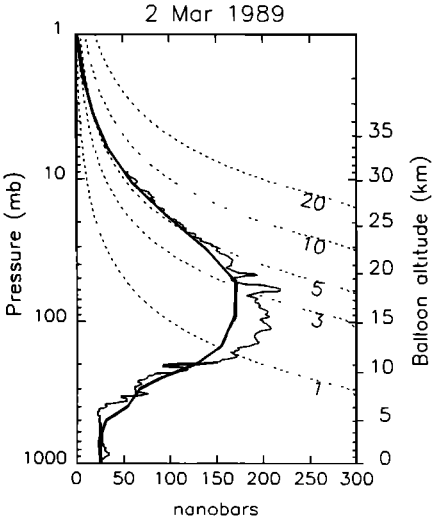

Fig. 17*e*

Fig. 17. Ozonesonde data and model profiles at Heiss Island (80°37°N, 58°3°E). (*a*) December 31, 1988. (*b*) January 25, 1989. (*c*) February 18, 1989. (*d*) February 19, 1989. (*e*) March 2, 1989.

the a priori assumption that the satellite data should provide a balanced budget.

The difficulties of calculating a balanced budget with the satellite data are most clearly revealed when attempting to calculate day-to-day changes. As with data [see *Douglass et al.*, 1985, *Douglass and Rood*, 1986], model fields separated by 24 hours give calculated changes that are frequently uncorrelated with observed changes. Once the spacing between model fields is reduced to 2–4 hours, the correlation between calculated and observed changes improves [*Geller et al.*, 1989]. Basically, there is so much transient structure in the fields that the assumption that a particular field is representative of 24 hours is wrong.

SUMMARY

The simulations presented here show a realistic representation of O_3 transport during winter. Perhaps the most obvious applications of this modeling technique are to satellite data. The satellite data will provide multiyear global data sets. The model can be run for these specific periods and produce a parallel constituent data set. Then direct comparison of the model to the observations and investigation of the differences will aid both data analysis and model development. The Upper Atmospheric Research Satellite will provide the next major data set for stratospheric science and will be much more complete than the LIMS data set.

The applications of this model, however, are not limited to satellite applications. The model has shown a capability to simulate synoptic events with accuracy. It has been shown to reproduce many of the characteristics of the AASE data. Therefore the model is a useful tool for evaluating how representative local variability is of zonal mean or global conditions. Since the transport is representative of real stratospheric states, the model can be used more confidently than most to assess the placement of ground-based stations and the impact of future aircraft missions.

Furthermore, even with the limited assimilation data sets currently available, the model can find applications to as-

sessment and trend studies. It can help quantify, with a higher degree of confidence than previously possible, the dynamical component of the interannual variability. It can also be directly applied to problems of fundamentally 3D processes. Such problems include the breakup of the polar vortex and its impact on middle latitudes and stratospheric-tropospheric exchange. Because of the skill that the model has exhibited in upper tropospheric, lower stratospheric transport, it will be a key tool in our current effort to assess the impact of high-speed stratospheric aircraft.

Acknowledgments. The authors would like to thank two anonymous reviewers for their helpful comments and William Lewis for sharing his knowledge of Pia Zadora's opus and world view. Stratospheric General Circulation with Chemistry Project at NASA GSFC contribution 60.

REFERENCES

Baker, W. E., S. C. Bloom, J. S. Woollen, M. S. Nestler, E. Brin, T. W. Schlatter, and G. W. Brantstator, Experiments with a three-dimensional statistical objective analysis scheme using FGGE data, *Mon. Weather Rev.*, *115*, 272–296, 1987.

Douglass, A. R., and R. B. Rood, Derivation of photochemical information near 1 mbar from ozone and temperature data, *J. Geophys. Res.*, *91*, 13,153–13,166, 1986.

Douglass, A. R., R. B. Rood, and R. S. Stolarski, Interpretation of ozone temperature correlations, 2, Analysis of solar backscattered ultraviolet ozone data, *J. Geophys. Res.*, *90*, 10,693–10,708, 1985.

Douglass, A. R., C. H. Jackman, and R. S. Stolarski, Comparison of model results transporting the odd nitrogen family with results transporting odd nitrogen species, *J. Geophys. Res.*, *94*, 9862–9872, 1989.

Douglass, A. R., R. B. Rood, R. S. Stolarski, M. R. Schoeberl, M. H. Profitt, J. J. Margitan, M. Loewenstein, J. R. Podolske, and S. E. Strahan, Global three-dimensional constituent fields derived from profile data, *Geophys. Res. Lett.*, *17*, 525–529, 1990.

Fahey, D. W., S. Solomon, S. R. Kawa, M. Loewenstein, J. R. Podolske, S. E. Strahan, and K. R. Chan, A diagnostic for denitrification in the winter polar stratospheres, *Nature*, *345*, 698–702, 1990.

Fritts, D. C., and R. A. Vincent, Mesosphere momentum flux studies at Adelaide, Australia: Observations and gravity wave-tidal interaction model, *J. Atmos. Sci.*, *44*, 605–619, 1987.

Geller, M. A., Modeling the middle atmosphere circulation, in *Dynamics of the Middle Atmosphere*, edited by J. R. Holton and T. Matsuno, pp. 467–500, D. Reidel, Hingham, Mass., 1984.

Geller, M. A., R. B. Rood, and J. A. Kaye, A strategy for using general circulation models and satellite data for improving understanding of the stratosphere, paper presented at the International Symposium on Middle Atmosphere Studies, Sci. Comm. on Solar Terr. Phys. (SCOSTEP), Dushanbe, USSR, Nov. 12–19, 1989.

Grose, W. L., J. E. Nealy, R. E. Turner, and W. T. Blackshear, Modeling the transport of chemically active constituents in the stratosphere, in *Transport Processes in the Middle Atmosphere*, edited by G. Visconti and R. Garcia, pp. 229–250, D. Reidel, Hingham, Mass., 1987.

Hayashi, Y., D. G. Golder, J. D. Mahlman, and S. Miyahara, The effect of horizontal resolution on gravity waves simulated by the GFDL "SKYHI" general circulation model, *Pure Appl. Geophys.*, *130*, 421–443, 1989.

Kaye, J. A., and R. B. Rood, Chemistry and transport in a three-dimensional stratospheric model: Chlorine species during a simulated stratospheric warming, *J. Geophys. Res.*, *94*, 1057–1083, 1989.

Leovy, C. B., C.-R. Sun, M. Hitchman, E. E. Remsberg, J. M. Russell III, L. L. Gordley, J. C. Gille, and L. V. Lyjak, Transport of ozone in the middle stratosphere: Evidence for planetary wave breaking, *J. Atmos. Sci.*, *42*, 230–246, 1985.

Loewenstein, M., J. R. Podolske, K. R. Chan, and S. E. Strahan, N_2O as a dynamical tracer in the Arctic vortex, *Geophys. Res. Lett.*, *17*, 477–480, 1990.

Mahlman, J. D., and W. J. Moxim, Tracer simulation using a global general circulation model: Results from a mid-latitude instantaneous source experiment, *J. Atmos. Sci.*, *35*, 1340–1374, 1978.

Mahlman, J. D., and L. Umscheid, Dynamics of middle atmosphere: Successes and problems of the GFDL SKYHI general circulation model, in *Dynamics of the Middle Atmosphere*, edited by J. R. Holton and T. Matsuno, pp. 501–525, D. Reidel, Hingham, Mass., 1984.

Mahlman, J. D., and L. Umscheid, Comprehensive modeling of the middle atmosphere: The influence of horizontal resolution, in *Transport Processes in the Middle Atmosphere*, edited by G. Visconti and R. Garcia, pp. 251–266, D. Reidel, Hingham, Mass., 1987.

McRea, G. J., W. R. Goodin, and J. H. Seinfeld, Numerical solution of the atmospheric diffusion equation for chemically reacting flows, *J. Comput. Phys.*, *45*, 1–42, 1982.

Mied, R. P., and G. J. Lindemann, Mass transfer between Gulf Stream rings, *J. Geophys. Res.*, *89*, 6365–6372, 1984.

Newman, P. A., L. R. Lait, M. R. Schoeberl, R. M. Nagatani, and A. J. Krueger, Meteorological atlas of the northern hemisphere lower stratosphere for January and February 1989 during the Airborne Arctic Stratospheric Expedition, *NASA Tech. Memo.*, *4145*, 1989.

Prather, M. J., Numerical advection by conservation of second-order moments, *J. Geophys. Res.*, *91*, 6671–6681, 1986.

Randel, W. J., The evaluation of winds from geopotential height data in the stratosphere, *J. Atmos. Sci.*, *44*, 3097–3120, 1987.

Remsberg, E. E., R. J. Kurzeja, K. V. Haggard, J. M. Russell III, and L. L. Gordley, Description of data on the Nimbus 7 LIMS map archive tape, *NASA Tech. Pap.*, *2625*, 1986.

Rind, D., R. Suozzo, and N. K. Balachandran, The GISS global climate–middle atmosphere model, II, Model variability due to interactions between planetary waves, the mean circulation, and gravity wave drag, *J. Atmos. Sci.*, *45*, 371–386, 1988.

Rood, R. B., Numerical advection algorithms and their role in atmospheric transport and chemistry models, *Rev. Geophys.*, *25*, 71–100, 1987.

Rood, R. B., D. Allen, W. Baker, D. Lamich, and J. Kaye, The use of assimilated stratospheric data in constituent transport calculations, *J. Atmos. Sci.*, *46*, 687–701, 1989.

Rood, R. B., J. A. Kaye, A. R. Douglass, D. J. Allen, S. D. Steenrod, and E. M. Larson, Wintertime nitric acid chemistry: Implications from three-dimensional model calculations, *J. Atmos. Sci.*, 2696–2709, 1990*a*.

Rood, R. B., P. A. Newman, L. R. Lait, D. J. Lamich, and K. R. Chan, Stratospheric temperatures during AASE: Results from STRATAN, *Geophys. Res. Lett.*, *17*, 337–340, 1990*b*.

Salby, M. L., Climate monitoring from space: Asynoptic sampling considerations, *J. Clim.*, *2*, 1091–1105, 1989.

Smagorinsky, J., General circulation experiments with the primitive equations, 1, The basic experiment, *Mon. Weather Rev.*, *91*, 99–164, 1963.

Takano, K., W. E. Baker, E. Kalnay, D. J. Lamich, J. E. Rosenfield, and M. A. Geller, Forecast experiments with the NASA/GLA stratospheric/tropospheric data assimilation system, *J. Meteorol. Soc. Jpn.*, *67*, 83–89, 1987.

van Leer, B., Towards the ultimate conservative difference scheme, II, Monotonicity and conservation combined in a second order scheme, *J. Comput. Phys.*, *14*, 361–370, 1974.

Wu, M.-F., M. A. Geller, J. G. Olson, and E. M. Larson, A study of global ozone transport and the role of planetary waves using satellite observations, *J. Geophys. Res.*, *92*, 3081–3097, 1987.

D. J. Allen, E. M. Larson, E. R. Nash, and J. E. Nielsen, Applied Research Corporation, 8201 Corporate Drive, Landover, MD.

A. R. Douglass, J. A. Kaye, and R. B. Rood, Atmospheric Chemistry and Dynamics Branch, Code 916, NASA Goddard Space Flight Center, Greenbelt, MD 20771.

M. A. Geller and Chi Y., Institute for Terrestrial and Planetary Atmospheres, State University of New York at Stony Brook, Stony Brook, NY 11794.

(Received August 20, 1990
revised November 15, 1990;
accepted November 16, 1990.)